

# Preliminary Evaluation of Surface Soil Response applying the H/V Spectral Ratio Technique to Microtremor Data within Dhaka City, Bangladesh

A. S. M. Maksud Kamal<sup>1)</sup>, S. Midorikawa<sup>2)</sup>, F. Yamazaki<sup>3)</sup>, and M. Ansary<sup>4)</sup>

1) Graduate student, Department of Built Environment, Tokyo Institute of Technology, Japan

2) Professor, Department of Built Environment, Tokyo Institute of Technology, Japan

3) Professor, Department of Urban Environment Systems, Chiba University, Japan

4) Associate Professor, Civil Engineering Department, BUET, Bangladesh

[kamal@enveng.titech.ac.jp](mailto:kamal@enveng.titech.ac.jp), [smidorik@enveng.titech.ac.jp](mailto:smidorik@enveng.titech.ac.jp), [yamazaki@tu-chba-u.ac.jp](mailto:yamazaki@tu-chba-u.ac.jp), [ansaryma@yahoo.com](mailto:ansaryma@yahoo.com)

**Abstract:** The geomorphological map of Dhaka city area with eighteen geomorphic units and four categories of landfills created by the authors previously employed as a major source of data used in this study. Data compiled from 140 boreholes provided information that allowed characterization of nine of the geomorphic units under analysis in terms of representative soil profiles and SPT-N values. Further analysis of overall shape of the SPT-N curves corresponding to these representative soil profiles suggested the possibility of regrouping them into four general patterns. Estimation of the site response through the evaluation of the predominant periods and corresponding amplification factors relied on the application of the horizontal to vertical spectral (H/V) technique employing 58 microtremor recordings distributed over twelve of the geomorphic units. Consideration of the similarity of the overall shape of the resulting transfer functions, predominant periods, and maximum amplification ratios suggested classification of the sites into three typical patterns. These H/V patterns displayed good correlation with the derived representative soil profiles. The compilation of a more extensive microtremor and borehole dataset covering all geomorphic units proved necessary for the further precise development of this work.

## 1. INTRODUCTION

The infrequent occurrence of destructive earthquakes does not permit the compilation of enough data to support the estimation of the distribution of damages in the future. To overcome this lacking, different authors proposed the use of alternative sources of excitation, such as, distant earthquakes, small near earthquakes, explosions, aftershocks and microtremors. The use of microtremors, an idea pioneered by Kanai *et. al.* (1954) turns into one of the most appealing approaches in site effects studies, due to its relatively low economic cost, and the possibility of recordings without strict spatial or time restrictions (Rodriguez and Midorikawa, 2002). The H/V spectral ratio technique of microtremors gained popularity in the early nineties, after the publication of several papers (Nakamura; 1989; Field and Jacob, 1993; Lermo and Shavez-Garcia, 1994) claiming the ability of this technique to estimate the site response of soft sedimentary deposits satisfactorily. The method is rather attractive in developing countries characterized by a moderate seismicity, where only very limited resources are available for seismic hazard studies.

Bangladesh is a country characterized by a moderate seismicity with almost no resources is available for large scale seismic hazard studies. The objective of this study was to evaluate the site response using H/V spectral ration of microtremors in terms of peak period and corresponding amplification within Dhaka city area (Figure-1), Bangladesh. This work was important for the nation, as a recent study conducted by Cardona *et. al* (2001) on twenty cities of

the world showed Dhaka appeared to have one of the highest values of earthquake disaster risk index (EDRI) mainly due to its inherent vulnerability of building infrastructures, high population density and poor emergency response and recovery capacity. Dhaka is positioned in the central part of Bangladesh, on a northwest-southeast elongated and southeastward tilted tectonically uplifted Pleistocene terrace. Regionally, Bangladesh is a part of the Bengal Basin, originated as a result of intra-plate movements involving the Indian, Tibetan and Burmese plates between Cretaceous to Holocene period.

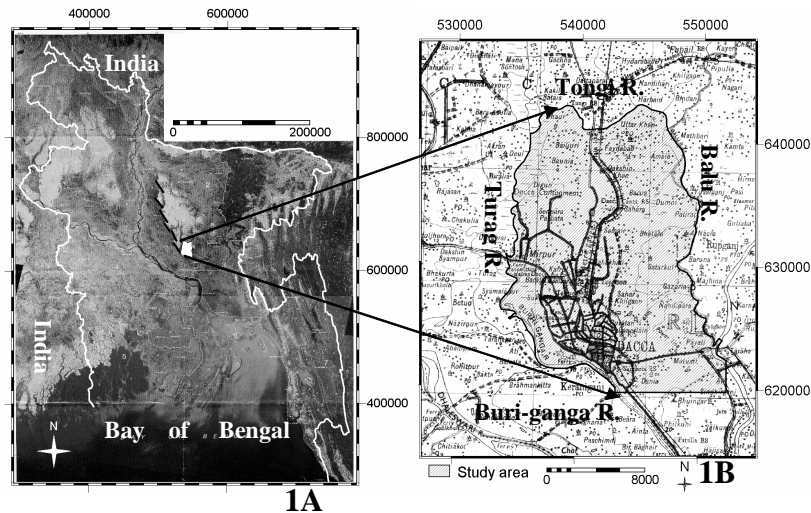


Figure 1A): Study area in white polygon on a Landsat TM mosaic of Bangladesh, 1B): Dhaka city area within the four river system as shown on Bangladesh topographic map no. 791

## 2. DATA USED

The geomorphological map of Dhaka city with eighteen units and four categories of thickness of the landfills (Figure 2) were created by the authors (Kamal and Midorikawa, 2003), through the combined analysis of old aerial photographs acquired in 1954, borehole data, and satellite images of Landsat TM<sup>+</sup> of bands (30 m resolution) 5, 4 and 3 and IRS-1D PAN (5.8 m resolution) taken in 2002 and 2000 respectively was used a major source of data in this study. The soil profiles of 140 boreholes with their SPT-N value curves were compiled and subsequently simplified them into patterns. Fifty-eight microtremors recording was measured at the ground surface with a three components velocity meter and processed to derive their spectral ratios (H/V). The H/V spectral ratio curves were analyzed and differentiated into three patterns. A simple flow chart of the materials and procedures used in this study shown in Figure 3:

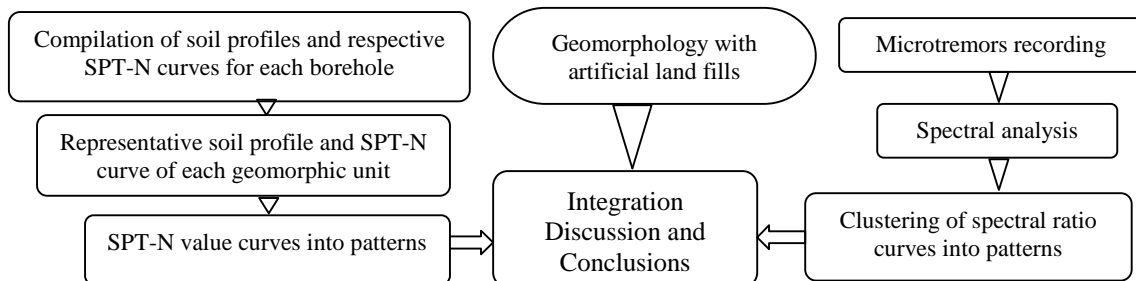
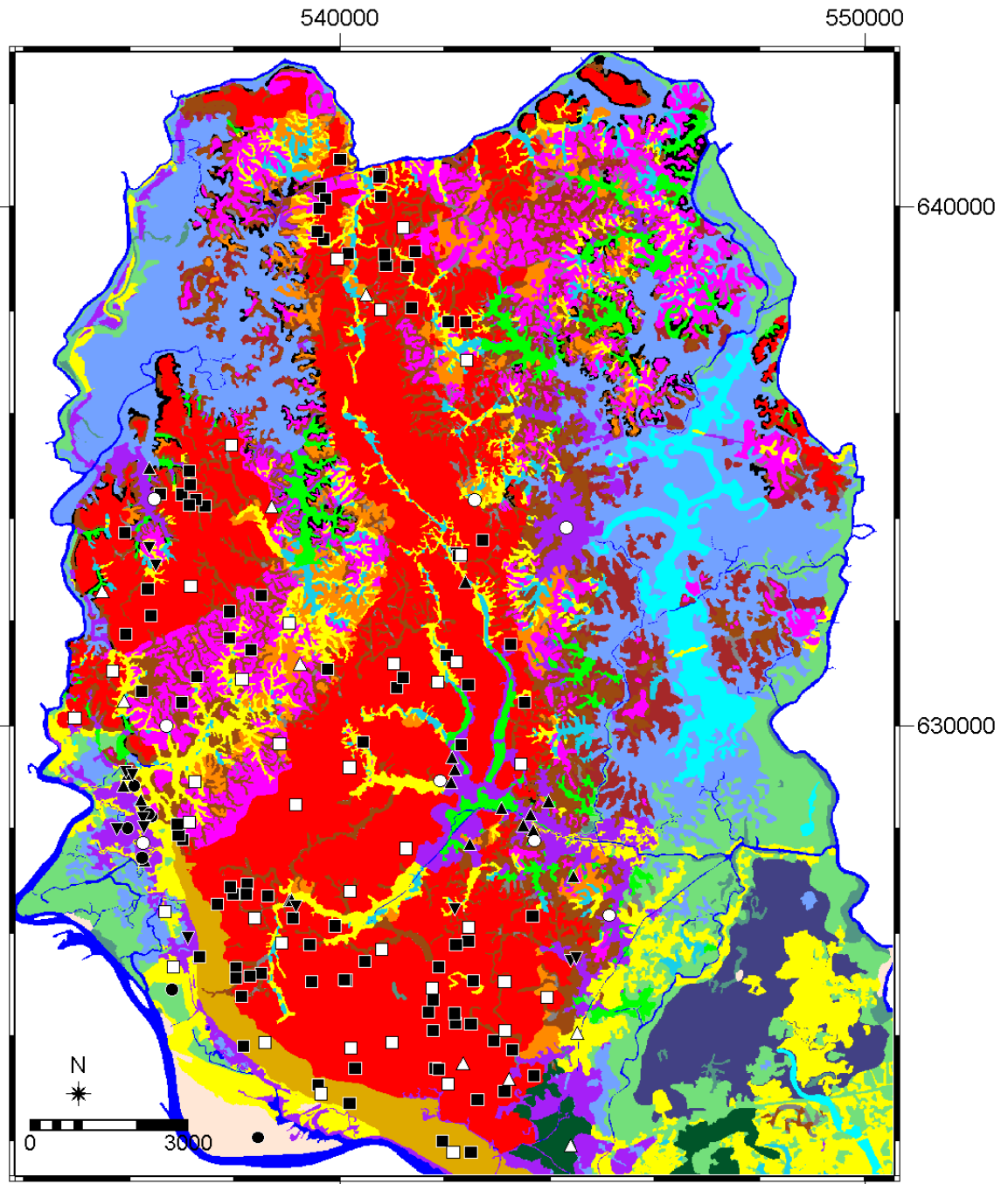


Figure 3: Simple flowchart of methodology

In the 'integration, discussion and conclusion' scheme, we overlaid the sites of the derived patterns of both boreholes and microtremors as the point information on the geomorphological map and examined the correlation among them.



**LEGEND**

- |  |  |
|--|--|
| <span style="color: cyan;">■</span> Abundant channel bed                             | <span style="color: brown;">■</span> Moderately thin fill                    |
| <span style="color: green;">■</span> Deep alluvial valley                            | <span style="color: orange;">■</span> Old natural levee                      |
| <span style="color: blue;">■</span> Deep marshy land                                 | <span style="color: white;">■</span> Pointbar/sand bar                       |
| <span style="color: black;">■</span> Gently sloping erosional terrace edge           | <span style="color: darkgreen;">■</span> Relatively old inactive flood plain |
| <span style="color: red;">■</span> Higher Pleistocene terrace                        | <span style="color: blue;">■</span> River system                             |
| <span style="color: darkred;">■</span> Highly erosional lower Pleistocene terrace    | <span style="color: grey;">■</span> Shallow alluvial valley                  |
| <span style="color: teal;">■</span> Inundated abundant channel                       | <span style="color: darkblue;">■</span> Shallow marshy land                  |
| <span style="color: cyan;">■</span> Moderately deep alluvial valley                  | <span style="color: purple;">■</span> Thick fill                             |
| <span style="color: orange;">■</span> Moderately erosional lower Pleistocene terrace | <span style="color: lightgrey;">■</span> Thin fill                           |
| <span style="color: magenta;">■</span> Moderately high Pleistocene terrace           | <span style="color: lightgreen;">■</span> Younger active floodplain          |
| <span style="color: yellow;">■</span> Moderately thick fill                          | <span style="color: darkgreen;">■</span> Younger natural levee               |

**SPT-N value based Pattern**

- |  |  |
|--|--|
| <span style="color: black;">■</span> Pattern-1 | <span style="color: black;">●</span> Pattern-3 |
| <span style="color: black;">▲</span> Pattern-2 | <span style="color: black;">▼</span> Pattern-4 |

**Spectral Ration-based Pattern**

- |  |  |
|--|--|
| <span style="color: black;">□</span> Pattern-1 | <span style="color: black;">○</span> Pattern-3 |
| <span style="color: black;">△</span> Pattern-2 |  |

Figure 2: Geomorphological map with Landfills. Both the patterns derived from SPT-N values of boreholes and spectral-ratios of microtremors were superimposed in this map.

### 3. BOREHOLE DATA ANALYSIS

We compiled the soil-profile and SPT-N value curves of 140 boreholes which were randomly distributed on the nine geomorphic units out of eighteen. All the SPT-N curves of a geomorphic unit were overlaid in a plot which provided the information of the representative soil profiles and corresponding SPT-N value of that geomorphic unit. Figure 4 below showed the representative soil profiles with SPT-N curves of the nine investigated geomorphic units.

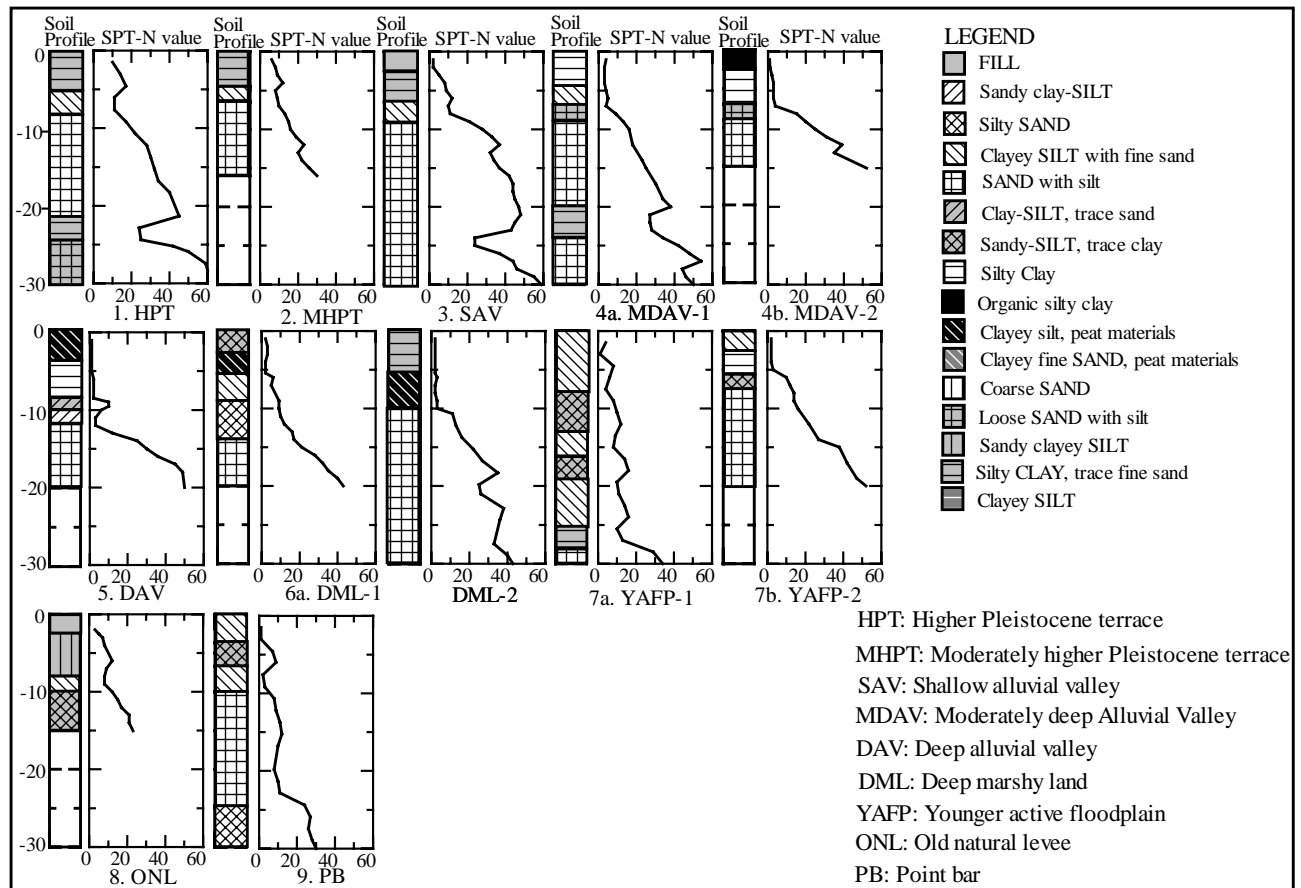


Figure 4: The representative soil profiles and SPT-N value of boreholes

In Figure 4, some geomorphic units showed more than one representative soil profiles. For instance, the younger active floodplain showed two representative soil profiles plotted as YAFF-1 and YAFF-2. The demonstration of SPT-N value curves of the boreholes of younger active floodplain justified two distinct appearances of YAFF-1 and YAFF-2, named as ‘category 1’ and ‘category 2’ respectively as shown in Figure 5. Thus, 140 boreholes of nine geomorphic units came-out into thirteen representative soil profiles and corresponding SPT-N value curves.

To investigate the relationship among the geomorphic units and to find-out the possibility in order to further simplify the thirteen representative soil profiles, we overlaid their SPT-N curves in a plot (Figure 6). It was observed that some SPT-N value curves closely correspond with each other. As an example, the curve of Higher Pleistocene terrace showed its close association with the curves of Moderately high Pleistocene terrace, Old natural levee and Shallow alluvial valley. Thus, based on the close association of representative SPT-N value curves, we grouped these four geomorphic units into a ‘pattern’. The thirteen representative soil profiles with SPT-N value curves, thus, simplified into four different patterns (Figure 7) for the nine geomorphic units of the study area. The association of the derived patterns with the geomorphic units was given below:

Pattern-1: The geomorphic unit of Higher Pleistocene terrace, Moderately higher Pleistocene terrace, Old natural levee and Shallow alluvial Valley.

Pattern-2: Category-2 of Deep marshy land, category-2 of Moderately deep alluvial valley and Deep alluvial valley.

Pattern-3: Category-1 of younger active floodplain and Point bar deposits.

Pattern-4: Category-1 of Moderately deep alluvial valley, Category-1 of deep marshy land and category-2 of Younger active floodplain.

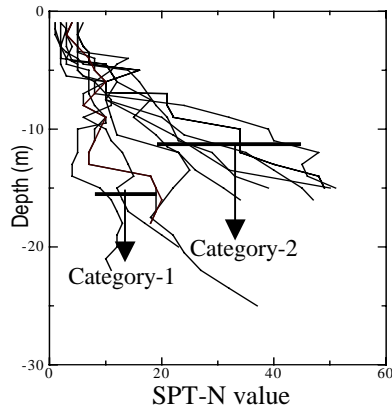


Figure 5: SPT-N value curves of category-1 and 2 of *Younger active floodplain*

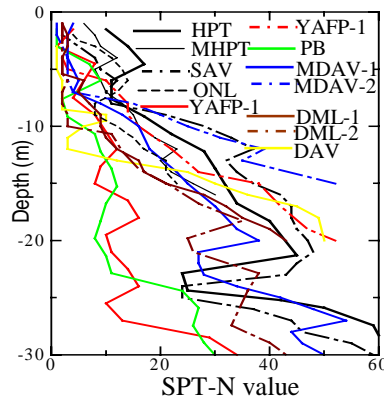


Figure 6: Thirteen representative SPT-N value curves of nine geomorphic units

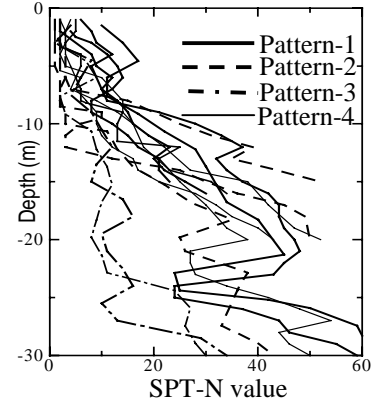


Figure 7: SPT-N value curves of four different patterns

#### 4. SPECTRAL ANALYSIS FOR H/V RATIOS OF MICROTREMORS

As mentioned before, 58 microtremors records were measured on twelve geomorphic units. Each record comprises of three components, viz., EW, NS and UD. For spectral analysis we took three noise-free portions of 20.48s of the recordings as the instrumental sampling frequency was 100Hz. However, to determine at which frequency of the spectrum, the sedimentary packages caused the larger amplifications we applied first Fourier transform on the time domain records, then smoothed the corresponding spectra and finally applied the spectral ratio (H/V) technique to derive transfer functions. The applied sequences were given below:

(1) At first, we calculated the Fourier spectra of the two horizontal and the vertical components. As the Fourier spectra of the two horizontal components looked alike, their horizontally combined spectra were calculated to obtain the maximum Fourier amplitude spectrum as a complex vector in the horizontal plane. While that of the UD component provided the vertical motion spectra.

(2) Smoothing of the spectra: After Fourier transformation, we digitally filtered the combined horizontal and vertical spectra applying a logarithmic window (Konno and Ohmachi, 1998; Rodriguez and Midorikawa, 2002) with a bandwidth coefficient equal to 15. This filtering technique was applied to reduce the distortion of peak amplitudes.

(3) Calculation of the soil response functions: The smoothed combined horizontal spectrum was divided with the vertical counterpart (H/V) which provided the desired predominant period and corresponding amplification factor of the investigated portions (20.48s) of records.

(4) After calculating three sets of the H/V ratios at each site, they were normalized to obtain a relatively non-biased site specific H/V ratio.

All the 58 records of microtremors were analyzed to obtain the predominant periods and corresponding amplification factors of the sites following the above sequences of analyses using a microtremor record measured on the Higher Pleistocene terrace as shown in Figure 8. From the tri-axial waveform W, three noise-free portions A, B, C having 20.48s long were selected for analysis in Figure 8. In the plots A(f), B(f), and C(f), the horizontal to vertical motion Fourier spectra were shown after smoothing by logarithmic window (width coefficient  $b=15$ ). The plots

D, E and F showed the soil response functions, where as, G represented the normalized H/V ratios after averaging D, E and F.

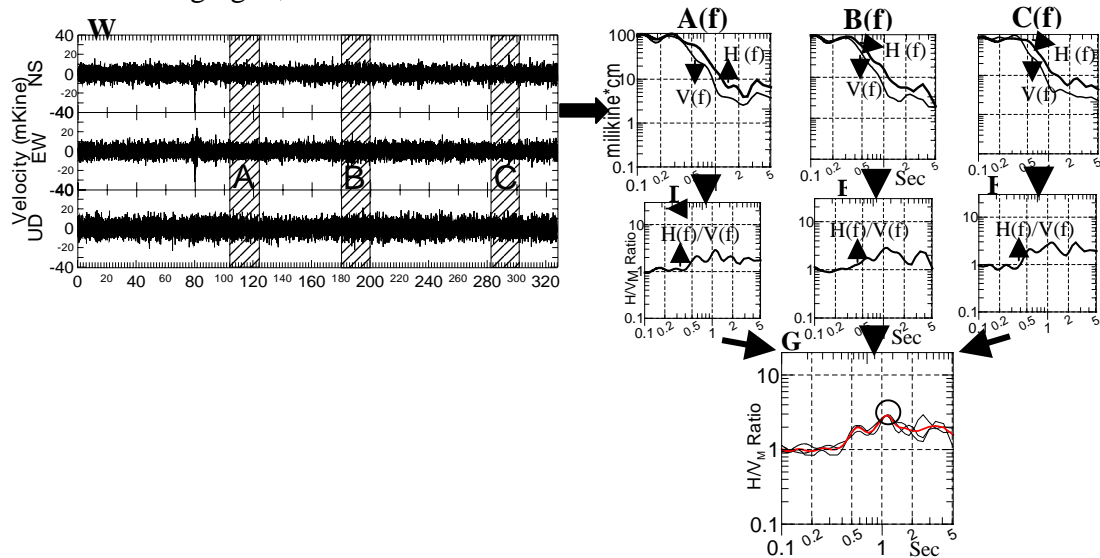


Figure 8: Flow of calculation process applied to obtain the transfer functions (H/V ratios).

The circle on the H/V curves in G showed the predominant period 1.13s and corresponding amplification factor 2.87 after averaging. The predominant period indicates the frequency of the spectrum under which the near-surface soft sediment amplifies the earthquake ground motion, which is often referred as the site effects. The degree of damage caused by earthquake shaking is larger when the predominant period of the sites appears near the period of the structure.

## 5. PATTERN RECOGNITION OF H/V CURVES

We observed that some of the H/V curves looked alike in shape even their measuring sites were located on different geomorphophic units. So, in order to increase the simplicity of the analysis, we classified the fifty-eight H/V spectral ratio curves of twelve geomorphophic units into the cluster of three ‘patterns’ (Figure 9) based upon: (1) the shape of the overall amplification spectra within the frequency range of interest; and (2) The coincidence between predominant periods and maximum spectral ratios. The descriptions of the patterns were as follows:

Pattern 1: We observed that the amplification spectra of 39 sites belonging to the six geomorphophic units viz., Higher Pleistocene terrace, Moderately higher Pleistocene terrace, Old natural levee, Old inactive floodplain, Shallow Alluvial Valley and some sites on Younger active floodplain represented a unique shape and their predominant periods around 1.0s with a standard deviation of 0.13. We found that on Higher Pleistocene terrace, the amplification was less than 3, where as, on the other geomorphophic units of this pattern, the amplification factor fluctuates in an order of 3-5.

Pattern-2: There were nine sites in pattern 2 under five geomorphophic units, namely, Moderately erosional lower Pleistocene terrace, Gently sloping erosional terrace edge, Inundated abundant channel, and some sites on Moderately deep alluvial valley as well as Younger active floodplain. The predominant period in this pattern was rather higher, in an average of around 1.86s. In the five sites of first three geomorphophic units of this pattern the amplification factors were around 4, where as, in the four sites of the last two, the amplification factors were higher fluctuating around 6-7.5

Pattern-3: The sites of this pattern were located on eight thick soft sediments, belonging four geomorphophic units, namely, Deep marshy land, Deep alluvial valley, Moderately deep alluvial valley and Younger active floodplain. There were two mode of predominant period observed in

this pattern. The short period mode fluctuated around 0.56s where as long period mode showed a typical 1.57s. The amplification factors were observed around 3.25 and 3-6 in short and long period modes respectively. In the Figure 9 below, the amplification spectra of each pattern and their calculated average were shown.

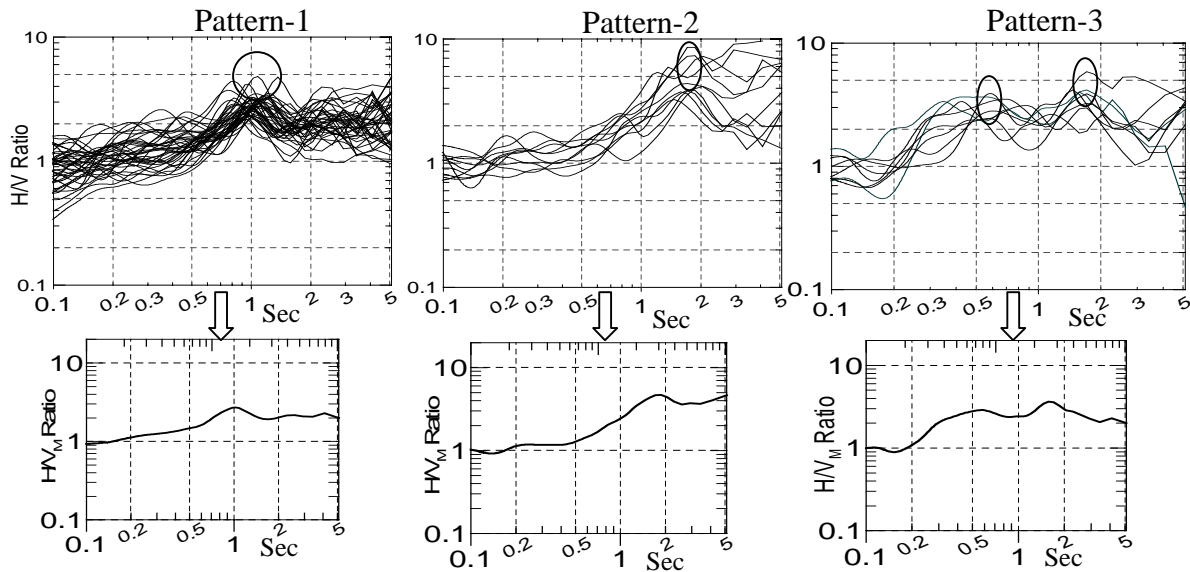


Figure 9: Spectral ratio curves and their normalized average shape as obtained from the analyses microtremors records on nine geomorphic units.

## 6. DISCUSSIONS AND CONCLUSIONS

We superimposed both the patterns derived from the borehole and microtremor data on the geomorphological map units as shown in Figure 2 in order to investigate whether the spatial distribution of sites under the SPT-N value-based patterns correspond with the spectra ration-based patterns.

It was observed that the spatial distribution of most the data comprising both the pattern-1 nicely corresponds with each other. The geomorphological units comprising these patterns included 99 boreholes and 39 microtremor data out of the total investigated amount of 140 and 58 respectively. The surface soil of these units was encountered comparatively stiffer than that of other geomorphic units. Although, the predominant period on these units were around 1.0 s but we observed the fluctuation of amplification in an order of 3-5 in the geomorphic units belonging to this pattern. This phenomenon can be explained by the inspections of Figure 10.

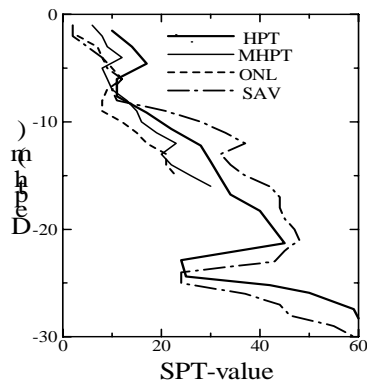


Figure 10: Four representative SPT-N value curves of pattern-1

The figure demonstrated that the SPT-N value of the top-soil of Higher Pleistocene terrace (HPT) was relatively higher than that of other geomorphic units of this pattern. The legend of SPT-N value curves in Figure 10 was organized from top to bottom according to the decrease of surface soil stiffness of the respective geomorphic units. The HPT, MHPT, ONL and SAV stood for Higher Pleistocene terrace, Moderately high Pleistocene terrace, Old natural levee and Shallow alluvial valley respectively. According to legend, the surface sediments of Higher Pleistocene terrace was very stiff, where as, shallow alluvial valley and Old natural levee represented less stiffness in surface soils. The Moderately higher Pleistocene terrace stood in between the above mentioned three

geomorphic units. The variations in the stiffness from hard to relative softness of the surface soil would be responsible for the fluctuations of amplification factors in the geomorphic units of this pattern. The SPT-N based 'pattern-1' showed that other than the above mentioned four units, Old inactive floodplain and three sites of Younger active floodplain belong to this pattern. Due to the lacking of borehole data, we could not correlate this pattern with SPT-N value based pattern-1.

The pattern-3 of the microtremor seems to be corresponded with pattern-2 of boreholes. The spatial distribution of these patterns incurred the geomorphic units, namely, Deep marshy land, some sites of Deep alluvial valley and Moderately deep alluvial valley. The representative soil profile with SPT-N curves in figure 4 suggested that the sites of these patterns showed a good impedance contrast in the near-surface strata at a depth of around 10 m. We assumed that this near-surface velocity contrast was the responsible for the developments of first mode of peak around 0.56. Due to the shallow depth of borehole, we could not explain the reason of another peak around 1.57 s. The amplification factors fluctuated in an order of 4-7, such a fluctuation of amplification was difficult to explain using this small amount of preliminary dataset.

The pattern-2 of microtremor did not show any specific relation with the borehole patterns. The pattern 3 and 4 of the boreholes included the sites which were under the geomorphic units of younger active floodplain, Point bar, Moderately deep alluvial valley and Deep marshy land. The representative soil profile showed the intercalation of many sub-soil strata in the sites of these patterns.

The amount of the data under the spectral ratio-based patterns 2 and 3 and SPT-N value curve-based patterns 2, 3 and 4 were not sufficient enough in this preliminary stage to draw a conclusion about their relationship. These spatial ratio-based and SPT-N value curve-based patterns included 19 and 41 sites of investigation. The compilation of a more extensive microtremor and deep borehole (more than 30 m depth) dataset covering all geomorphic units proved necessary from this preliminary investigation to draw the convincing conclusion among the relationship in the patterns of microtremor and boreholes with respect to geomorphic units.

## References:

- Kanai, K. Tanaka, T. and Osada K. (1954), "Measurements of Micro-tremors 1. *Bulletin Earthquake Research Institute*, Tokyo University, 32, 199-210.
- Rodriguez, V. S. H. and Midorikawa, S. (2002), "Applicability of the H/V Spectral Ratio of Microtremors in Assessing Site Effects on Seismic Motion," *Earthquake Engineering and Structural Dynamics*, 31, 261-279.
- Nakamura, Y. (1989), "A Method for Dynamic Characteristics of Sub-surface Using Microtremors on the Ground Surface," *Quick Report of Railway Technical Research Institute*, 30(1)-25-33 (in Japanese).
- Field, E. H. and Jacob K. H. (1993), "The Theoretical Response of Sedimentary Layers to Ambient Seismic Noise," *Geophysical Research Letter*, 20, 2925-2928.
- Lermo, J. and Chavez-Garccia, F. J. (1994), "Are Microtremors Useful in Site Response Evaluation?," *Bulletin of Seismological Society of America*, 84, 1350-1364.
- Cardona, C. Davidson, R. and Villacis, C. (1999), "Understanding Urban Seismic Risk Around the World- A Final Report on the Comparative Study," *A project of the United Nations RADIUS Initiative, IDNDR, published by Geo-Hazards International*.
- Kamal, A. S. M. M, and Midorikawa, S. (2003) "GIS-based Landfill Mapping of Dhaka City Area, Bangladesh, Using Remote Sensing Data," *Proceedings on the Second International Symposium on New Technologies for Urban Safety of Mega Cities in Asia*, University of Tokyo, Japan.
- Konno, K. and Ohmachi, T. (1998), "Ground-motion Characteristics Estimated from Spectral Ratio between Horizontal and Vertical Components of Microtremor," *Bulletin of the Seismological Society of America*, 88(1), 228-241.
- Rodriguez, V. H. S. and Midorikawa, S., (2003), "Comparison of Spectral Ratio Technique for Estimation of Site Effects Using Microtremor Data and Earthquake Motions Recorded at the Surface and in Boreholes," *Earthquake Engineering and Structural Dynamics*, 32, 1691-1714.